PFC/JA-88-8

Effects of Electron Prebunching on the Radiation Growth Rate of a Collective (Raman) Free Electron Laser Amplifier

C. Leibovitch,† K. Xu,†† and G. Bekefi

March 1988

Department of Physics and Research Laboratory of Electronics
Massachusetts Institute of Technology
Cambridge, Massachusetts 02139

†Permanent address: Applied Physics Dept., Scientific Div., Rafael Laboratory, P.O. Box 2250, Haifa 31021, Israel

††Permanent address: Chengdu Institute of Radio Engineering, Research Institute of Microwave Electronics, Chengdu, Sichuan, PRC

This work was supported by the National Science Foundation and the U.S. Air Force Office of Scientific Research.

Submitted for publication in: IEEE Journal of Quantum Electronics

EFFECTS OF ELECTRON PREBUNCHING ON THE RADIATION GROWTH RATE OF A COLLECTIVE (RAMAN) FREE ELECTRON LASER AMPLIFIER

C. Leibovitch,† K. Xu,†† and G. Bekefi

Department of Physics and Research Laboratory of Electronics
Massachusetts Institute of Technology
Cambridge, Massachusetts 02139

ABSTRACT

Experiments are reported on the effects of electron prebunching in a mildly relativistic, low current (200kV, 1A) free electron laser amplifier operating in the collective (Raman) regime at a frequency of ∿10GHz. Prebunching is established by injecting an electromagnetic wave into a bifilar helical wiggler and then transporting the bunched beam into a second magnetic wiggler region. The wave growth rate is deduced from measurements of the radiation intensity as a function of interaction length. Observations show that prebunching can increase the radiation growth rate manyfold as compared with a system without prebunching. Studies are presented both in the small signal (linear) regime, and in the nonlinear (saturated) regime.

†Permanent address: Applied Physics Dept., Scientific Div., Rafael Laboratory, P.O. Box 2250, Haifa 31021, Israel.

††Permanent address: Chengdu Institute of Radio Engineering, Research Institute of Microwave Electronics, Chengdu, Sichuan, People's Republic of China.

1. INTRODUCTION

The concept of prebunching electron beams has a long and venerable history; the klystron [1] is a famous example. Prebunching is also used to improve the performance of other sources of coherent radiation. It is used in traveling wave tubes (TWT) to suppress parasitic feedback oscillations caused by wave reflections at or near the output of the device [2]; and it has been used in traveling wave tubes and klystrons to achieve radiation at high frequencies by arranging for the bunched beam to emit on high harmonics [3]. In more recent applications, prebunching the beams in gyrotrons (the so-called gyroklystron configuration) can lead to improved efficiency [4]. In the case of free electron lasers (FEL), systems with prebunching are referred to as optical klystrons. The concept [5] has been employed successfully to increase the overall optical gain both at the fundamental [6] and at high harmonics [7]. Such gain enhancement is of particular importance at short wavelengths (visible and VUV) where FEL gains are of necessity small.

To date, experimental and theoretical studies of the optical klystron have been carried out in the low gain, single particle (Compton) regime applicable to very short radiation wavelengths (visible and ultraviolet) where electron beam energies, in excess of several hundred MeV are used. In contrast, our experiments are made at microwave frequencies using mildly relativistic electrons ($\sim$200keV). In this collective (Raman) regime, the gains are high and the effects of space charge cannot be neglected. We find that prebunching does indeed increase the growth rate of the radiation quite dramatically as compared with the case where prebunching has not been incorporated. We present our studies both in the small signal (linear) regime and in the nonlinear (saturated) regime.

2. EXPERIMENTAL ARRANGEMENT

In an optical klystron-like system, the region of prebunching and the region where the desired stimulated emission is to take place are separated spatially. To make the prebunching more rapid, an intervening dispersive element can also be inserted [5], [6], [7]. Thus, such configurations are quite unlike a conventional FEL where bunching and stimulated emission are fully spatially intermingled.

Figure 1 shows a schematic of our experiment. The accelerating potential is supplied by a Marx generator (Physics International Pulserad 615MR, which has a maximum capability of 500kV and 4kA). Since this accelerator does not use a pulse-forming network, the output voltage pulse is essentially that of a discharging capacitor bank with a shunt adjusted RC time constant of 10-100 μsec. The electron beam is generated by a thermionically emitting, electrostatically focused, Pierce-type electron gun (250kV, 250A) from a SLAC klystron (model 343). An assembly of focusing coils transports the electron beam into the drift tube. To insure good electron orbits, an aperture is inserted which limits the electron beam radius to r_b=0.245cm so that only the inner portion of the beam is used [7]. With this precaution, the energy spread of the beam entering the magnetic wiggler is $\Delta\gamma_{\parallel}/\gamma_{\parallel} \lesssim 0.003$ ($\gamma_{\parallel} = [1 - v_{\parallel}^2/c^2]^{-\frac{1}{2}}$).

The gun focusing coils guide the electron beam into a rectangular (0.40"×0.90") stainless steel evacuated drift tube which is also the waveguide for the electromagnetic radiation. The beam is contained by a uniform axial magnetic field $B_{\parallel}$ that has a power supply limited maximum of 7kG and a minimum of approximately 800G. Below this value, beam defocusing and deterioration occur. The net current entering the magnetic wiggler is in the range of 1-5A.

The 65 period circularly polarized magnetic wiggler has a period ℓ_w=3.5cm, a maximum amplitude B_w=1.0kG, and is generated by bifilar conductors. Since

the beam aperture limits the size of the beam to $r_b/\ell_w \simeq 0.07$, the wiggler field is close to that of an ideal wiggler. That is, the effects of the radial variation of the wiggler field and the presence of the off-axis components are usually small. At the wiggler entrance a slowly increasing field amplitude is produced by resistively loading the first six periods of the wiggler magnet [9].

The 2.7m long drift tube acts as a rectangular waveguide whose fundamental TE_{10} mode has a cutoff frequency of $\omega_c/2\pi = 6.6$GHz. Microwaves are launched onto the electron beam by a waveguide coupler (see Fig. 1). All our measurements are carried out at frequencies between 9 and 11GHz. At these frequencies the empty waveguide can support only the fundamental (TE_{10}) mode, all higher modes being evanescent.

Monochromatic radiation as high as 20kW is injected into the interaction region via the directional coupler. At low power levels ($\lesssim$10W) we use a CW traveling wave tube as the input source. At higher power levels we use a pulsed ($\sim$1μ) magnetron driver. Because of the low conductivity of the stainless steel waveguide, there is an RF power loss of $\sim$0.9dB/m, or a 3dB loss over the entire system length.

3. MEASUREMENTS

The interaction space is divided into two roughly equal lengths by means of a tungsten mesh stretched across the waveguide (see Fig. 1) and placed at an axial distance $z = z^* \simeq 115$cm from the wiggler entrance. The mesh is almost totally transparent ($\sim$94%) to the electron beam generated to the left of the mesh, but highly reflecting to the electromagnetic radiation incident upon it. Thus, the left-hand side can be viewed as the prebunching region where spatially growing bunches are induced by the conventional FEL mechanism. The bunched beam then traverses the mesh almost unhindered and immediately interacts with

the weak electromagnetic wave that has been allowed to pass through the mesh. (The mesh attenuation of the wave incident from the left equals 20.0dB.) Beyond the mesh the electromagnetic wave grows spatially, and additional bunching also occurs. We note that although the regions to the left and right of the mesh are geometrically almost indistinguishable from one another, they are very different in regard to the wave-particle interactions that occur there. To the far left the electrons generated by the electron gun enter the system uncorrelated in their phases; on the other hand, the electrons entering the right hand region are spatially phase correlated. The tightness of the bunches at $z=z^*$ depends on a number of system parameters such as the strength of the wiggler field, the electron beam energy and current, etc. The use of the mesh rather than an RF attenuator of finite axial extent, as is common in TWTs [2], minimizes the possibility of debunching with distance, as may well occur as a result of space charge repulsion and/or Landau damping [8] of the ponderomotive wave.

At the output end of the wiggler, a mica window transmits the linearly polarized radiation generated in the drift tube, where it is measured by means of standard calibrated crystal detectors. In order to determine the growth rate of the wave, the output intensity must be measured as a function of the length of the interaction region. This is accomplished by means of an axially movable horseshoe "kicker" magnet that deflects the electron beam into the waveguide wall at any desired position z, thereby terminating the interaction at that point. The position z can be chosen to be to the left or to the right of the tungsten mesh (situated at $z=z^*\simeq 115$cm).

Figure 2 shows how the RF output power P(z) varies with distance z for two different values of the wiggler strength B_w. We see that to the right of the mesh the power rises much more rapidly with z than to the left of the mesh; we ascribe this to the effect of electron prebunching. The phenomenon is quite

dramatic. For example, in the case of the B_w=100G wiggler field, the radiation growth rate $\Gamma(z<z^*) \equiv (1/P)dP/dz$ equals 6.9dB/m, whereas to the right of the mesh, $\Gamma(z>z^*)$=32dB/m. Note, however, that for our parameters, the gain G, namely the ratio of total output power to the total injected power (at z=0), is not improved relative to what G would have been in the absence of prebunching. The reason is the 23dB loss (20dB due to the mesh and 3dB due to finite waveguide conductivity) which has not been made up by the additional gain. However, we believe that a better choice of parameters and a better choice of geometry can overcome this deficiency of our experiment.

Figure 3 illustrates how the output power varies with wiggler strength B_w for two different positions of the magnetic "kicker". In Fig. 3(a) the kicker is placed just to the left of the mesh $z \lesssim z^*$. Here the variation of the output power with B_w is typically what one would expect from a conventional Raman FEL of that length [8]. Figure 3(b) shows how the output varies when the kicker is placed far to the right of the mesh. Here, the rapid rise of the output intensity is indicative of strong prebunching, and is followed by nonlinear saturation at high B_w.

Figure 4 shows how the power P(z) varies with z for three different values of the input power P_{in} ranging from 0.3W to 40W. The wiggler strength B_w is the same for all three values of P_{in}. It is seen that the growth rate Γ (given by the slopes of the curves) are virtually independent of the input power.

In the measurements shown in Figs. 2, 3, and 4 the input power is sufficiently small ($\lesssim$40W) so that nonlinear effect are largely absent (except for the case of large wiggler field amplitudes as seen in Fig. 3(b)). Figure 5 illustrates the system behavior when the input powers are large, and nonlinear saturation becomes dominant at quite small values of z. It is noteworthy

that the saturated output power does not change appreciably with increased input power, indicating that the saturated efficiency is virtually independent of the injected radiation intensity even when this is varied over a wide range from 25W to 20kW. In the saturated region, large synchrotron oscillations [10] are also clearly visible.

4. DISCUSSION

We have reported on the effects of prebunching in a Raman free electron laser amplifier, and observed large enhancements in the single pass growth rates Γ. Most of the observations were made using RF drivers that operate either CW or with microsecond long pulses. To verify that the measurements of Γ indeed represent single pass gain and are not marred by reflections (due to the presence of the mesh, for example) we also carried out a series of measurements in which the pulse length ($\sim$5ns) of the RF input was shorter than the round trip pass through the system.

To the left of the mesh, ($z<z^*$) the system behaves as one would expect from a conventional FEL operating in the Raman regime. Thus, when the wiggler field strength B_w is increased from 38G to 100G, (Fig. 2) the growth rate Γ ($z<z^*$) increases from 2.4dB/m to $\sim$6.9dB/m, which shows that $\Gamma(z<z^*) \propto B_w$, in agreement with expectations. Also, $\Gamma(z<z^*)$ is found to be independent of the input power P_{in} (Fig. 4) for sufficiently low input powers, such that nonlinear phenomena are unimportant. This is also in agreement with theory [8].

To the right of the mesh ($z>z^*$) the situation is different. When B_w is increased from 38G to 100G (a factor of 2.6), $\Gamma(z>z^*)$ increases from 6.3dB/m to 32dB/m (a factor of 5.1). However, growth rate $\Gamma(z>z^*)$ remains independent of the RF power input P_{in} (Fig. 4).

Our studies are in the nature of proof of principle experiments. To suppress parasitic oscillations in a Raman FEL device, one may want to replace

the tungsten mesh with a short attenuating section in the manner used in TWTs [2]. To improve the gain, when the gains are too low, one may want to insert a (dispersive) drift region between the buncher and the emitter [5], [6], [7] as is done in Compton-type FELs. In either case, improvements and system optimization require detailed numerical simulations which are described in a companion paper [10].

ACKNOWLEGEMENTS

This work was supported by the National Science Foundation and the U.S. Air Force Office of Scientific Research.

REFERENCES

[1] J.C. Slater, Microwave Electronics (D. van Nostrand 1950) p. 222.

[2] J.R. Pierce, Traveling Wave Tubes (D. van Nostrand 1950) chapter IX, pages 131-144; also S.Y. Liao, Microwave Devices and Circuits (Prentice Hall 1985) pp 220-224.

[3] M.D. Sirkis and P.D. Coleman, "The Harmodotron - a Megavolt Electronics Millimeter Wave Generator" J. Appl Phys. 28, 944-950 (1957).

[4] See for example T.M. Tran, B.G. Danly, K.E. Kreischer, J.B. Schutkeker, and R.J. Temkin, "Optimization of Gyroklystron Efficiency", Phys. Fluids 29, 1274-1281 (1986) and references therein.

[5] R. Coisson, "Optical Klystrons" in Particle Accelerators (Gordon and Breach 1981) Vol. II, pp 245-253, and references therein.

[6] M. Billardon, P. Elleaume, Y. Lapierre, J.M. Ortega, C. Bazin, M. Bergher, J. Marilleau, and Y. Petrov, "The Orsay Storage Ring Free Electron Laser: New Results", in Proceedings Seventh International Conference on Free Electron Lasers, E.T. Scharlemann and D. Prosnitz, Editors (North Holland 1986) pp 26-34.

[7] B. Kincaid, R.R. Freeman, A.M. Fauchet, G. Vignola, C. Pellegrini, and A. van Steenbergen, "The TOK Experiment", Proc. Nineth International Free Electron Laser Conference, Williamsburg, Virginia 1987.

[8] J. Fajans, G. Bekefi, "Measurements of Amplification and Phase Shift (Wave Refractive Index) in a Free-Electron Laser", Phys. Fluids 29, 3463-3469 (1986).

[9] J. Fajans, "End Effects of a Bifilar Magnetic Wiggler", J. Appl. Phys. 55, 43-50 (1984).

[10] J. Fajans, J.S. Wurtele, G. Bekefi, D.S. Knowles, and K. Xu, "Nonlinear Power Saturation and Phase (Wave Refractive Index) in a Collective Free-Electron Laser Amplifier", Phys. Rev. Lett. 57, 579-582 (1986).

[11] J. Fajans and J.S. Wurtele Massachusetts Institute of Technology Plasma Fusion Center Report No. PFC/JA-88-9 (1988).

FIGURE CAPTIONS

Fig. 1. Schematic of the experimental setup.

Fig. 2. RF power output as a function of interaction length, for two different wiggler field amplitudes B_w; RF power input 3W; RF frequency 10.5GHz; electron beam energy 170keV; electron beam current ≈1A; axial guide magnetic field $B_{\parallel}$=1.55kG.

Fig. 3. RF power output as a function of wiggler field strength B_w; (a) just upstream from the mesh at z=100cm; (b) at the end of the wiggler. All other parameters are the same as in the caption to Fig. 1.

Fig. 4. RF power output as a function of interaction length, for three different values of RF input power. RF frequency 9.3GHz; electron beam energy 130keV; electron beam current ≈1A; wiggler field strength 100G; axial guide field $B_{\parallel}$=1.55kG.

Fig. 5. RF power output as a function of interaction length, showing nonlinear saturation effects. All other parameters are the same as in the caption to Fig. 4.

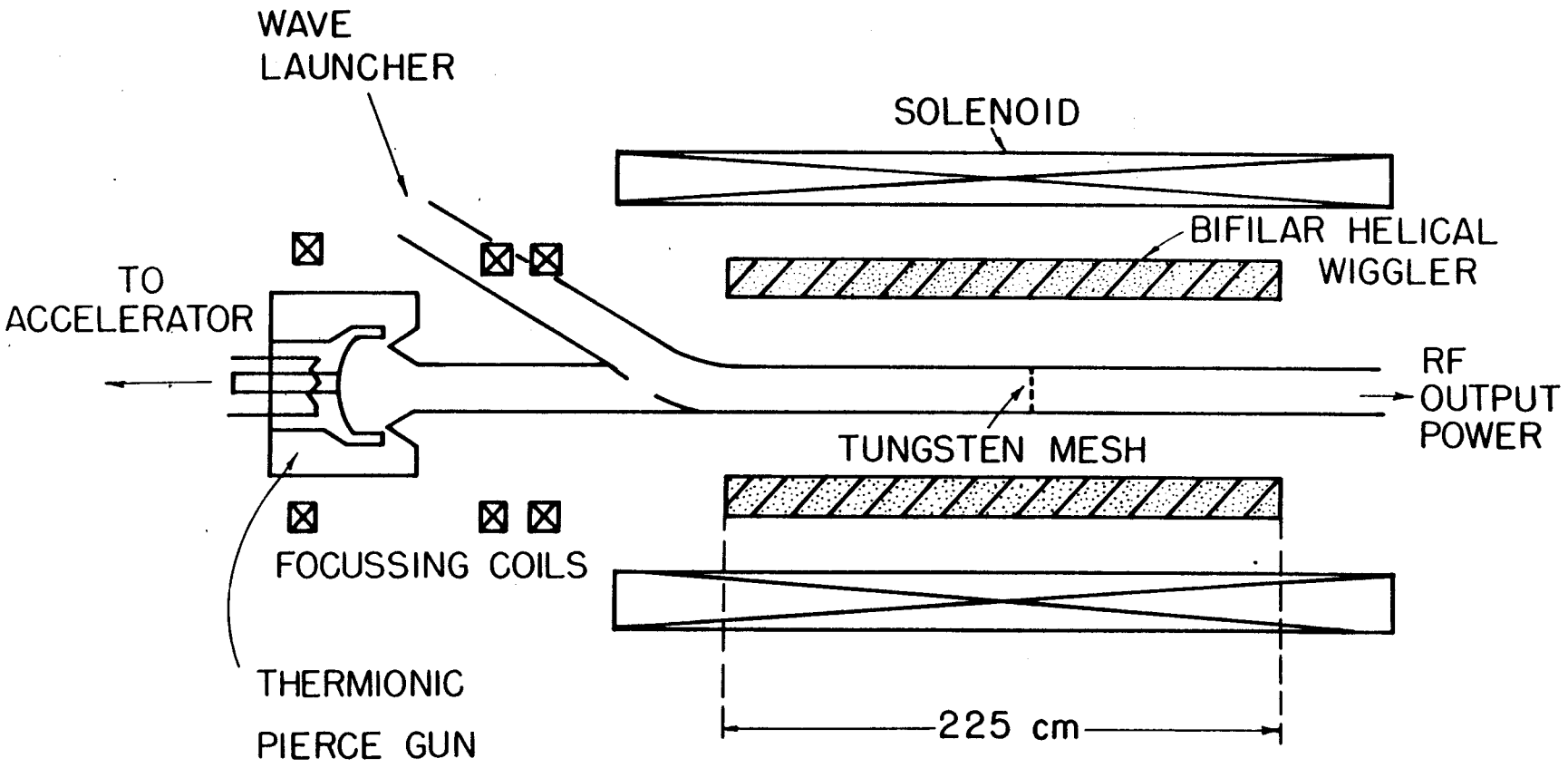

Fig. 1
Leibovitch, Xu, Bekefi

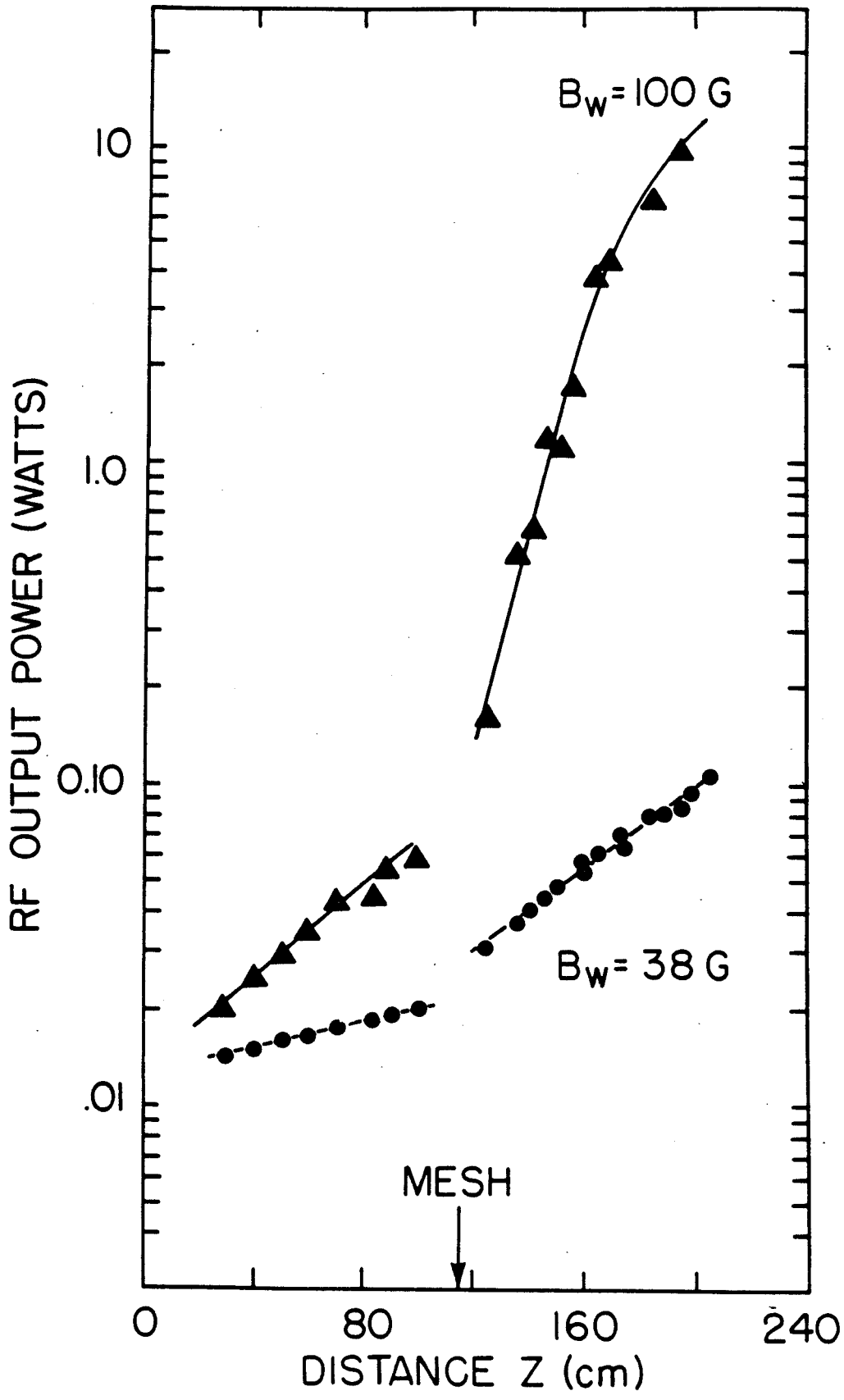

Fig. 2
Leibovitch, Xu, Bekefi

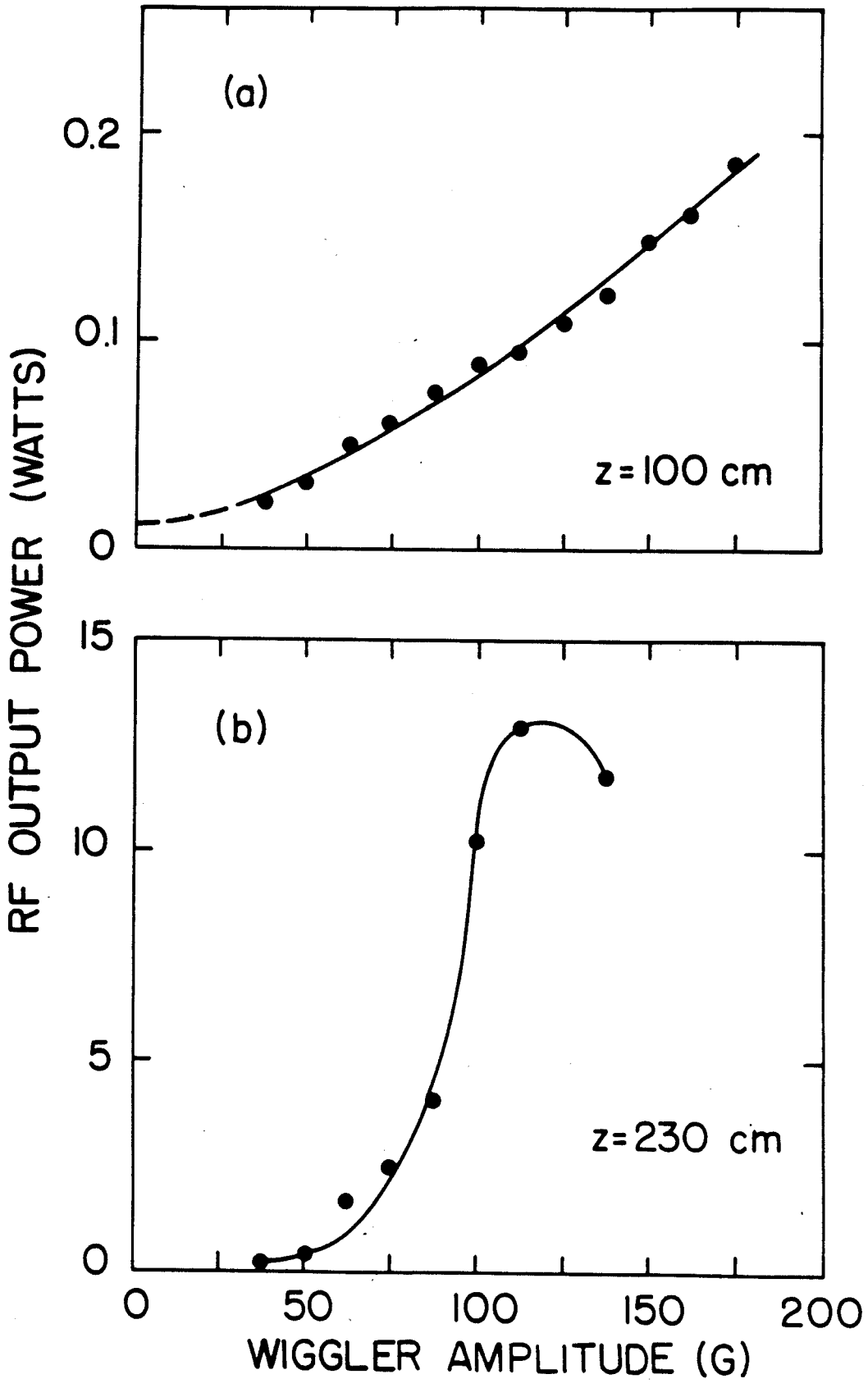

Fig. 3
Leibovitch, Xu, Bekefi

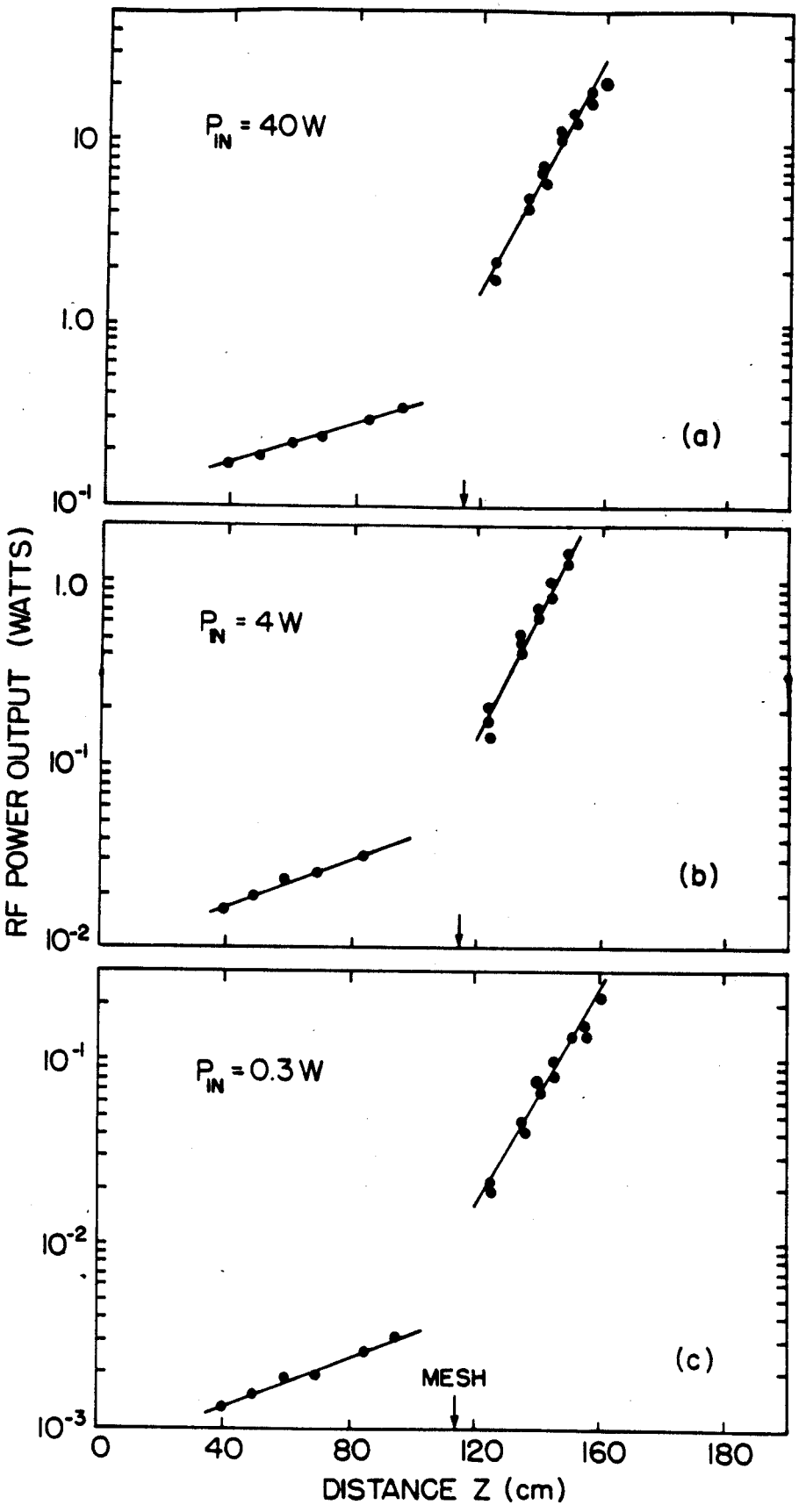

Fig. 4
Leibovitch, Xu, Bekefi

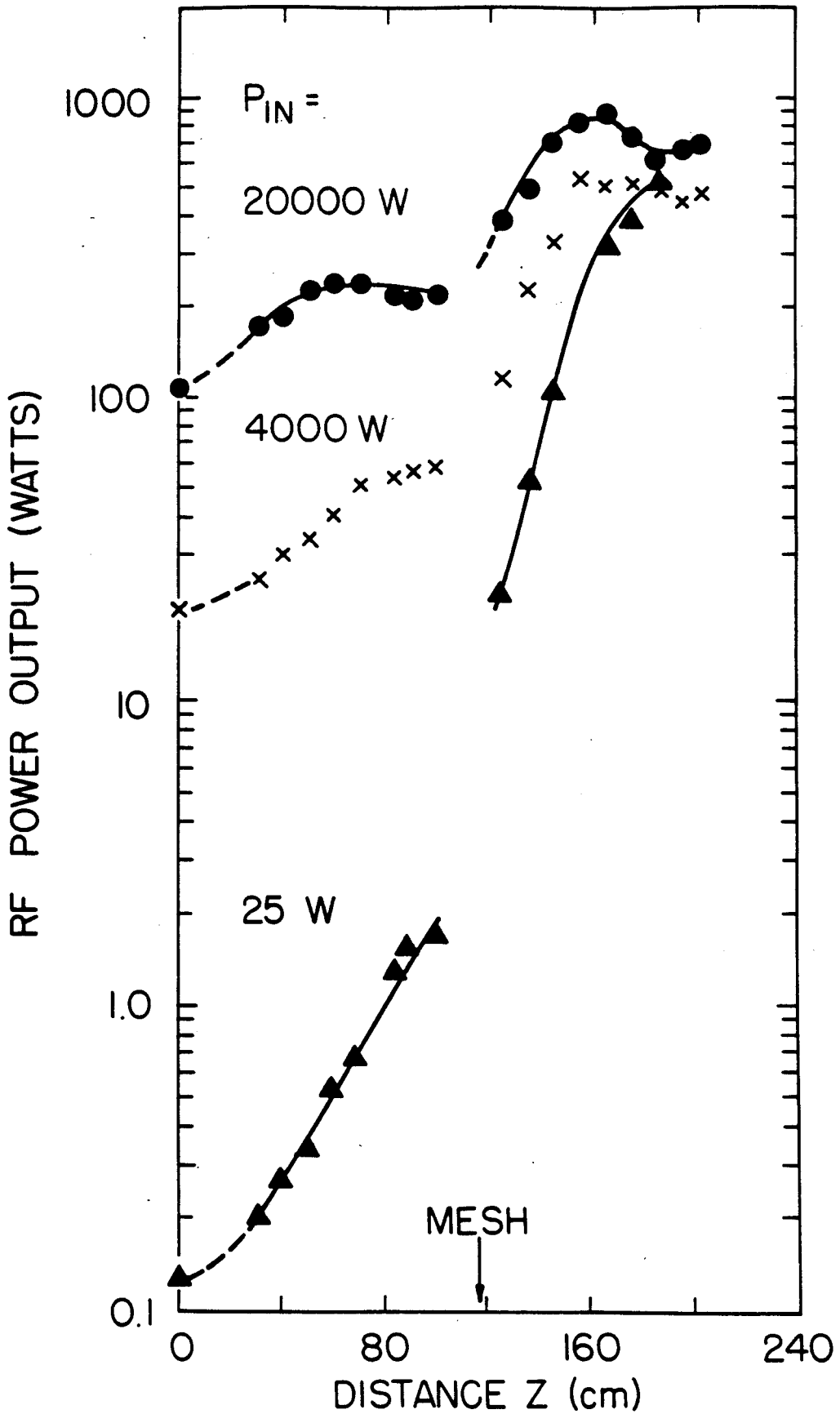

Fig. 5
Leibovitch, Xu, Bekefi